

Electronic Supplementary Information

Oxidomolybdenum complexes for acid catalysis using alcohols as solvents and reactants

Ana C. Gomes,^a Patrícia Neves,^a Luís Cunha-Silva,^b Anabela A. Valente,*^a
Isabel S. Gonçalves^a and Martyn Pillinger*^a

a Dr. A. C. Gomes, Dr. P. Neves, Dr. A. A. Valente, Prof. Dr. I. S. Gonçalves, Dr. M. Pillinger

Department of Chemistry, CICECO - Aveiro Institute of Materials
University of Aveiro

Campus Universitário de Santiago, 3810-193 Aveiro, Portugal
E-mail: atav@ua.pt (A.A.V.), mpillinger@ua.pt (M.P.)

b Dr. L. Cunha-Silva

REQUIMTE-LAQV, Departamento de Química e Bioquímica
Faculdade de Ciências, Universidade do Porto
4169-007 Porto, Portugal

Contents:

Figures S1 - S10 (pages S2 - S12): Supplementary Figures showing powder XRD patterns (Figs. S1 and S10), FT-IR data (Fig. S2), GC-MS data (Fig. S3), and additional crystallographic representations (Figs. S4-S9).

Additional crystallographic discussion (page S6): A description of the crystal packing arrangements for **2**, **4**·2EtOH and **4**·5CHCl₃.

Tables S1 - S7 (pages S13 - S17): Crystal and structure refinement data, selected bond lengths and angles, and hydrogen bonding geometries.

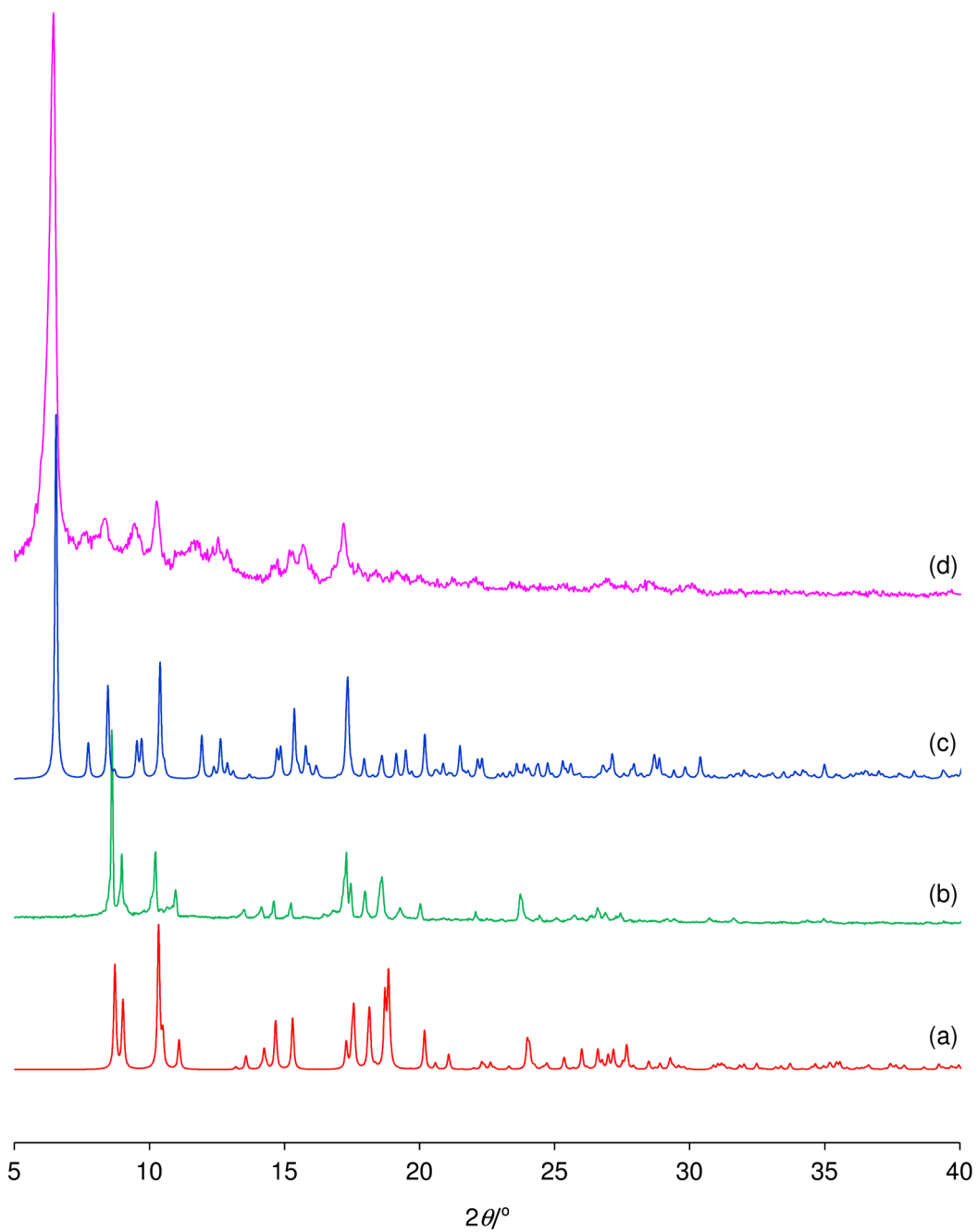


Fig. S1 Experimental powder X-ray diffraction patterns of (b) bordeaux precipitate obtained after vapour diffusion of pentane into the mother liquor obtained after reaction of complex **1** with ethanol under reflux and (d) bulk powder (**5**) obtained after reaction of **1** with *tert*-butanol under reflux. Simulated patterns calculated from single-crystal X-ray structure data are shown in (a) for complex **2** (this work) and in (c) for the hydrate **5**· $0.2\text{H}_2\text{O}$ (A. C. Gomes *et al.*, *Acta Crystallogr. Sect. E: Struct. Rep. Online*, 2011, **E67**, m1738-m1739).

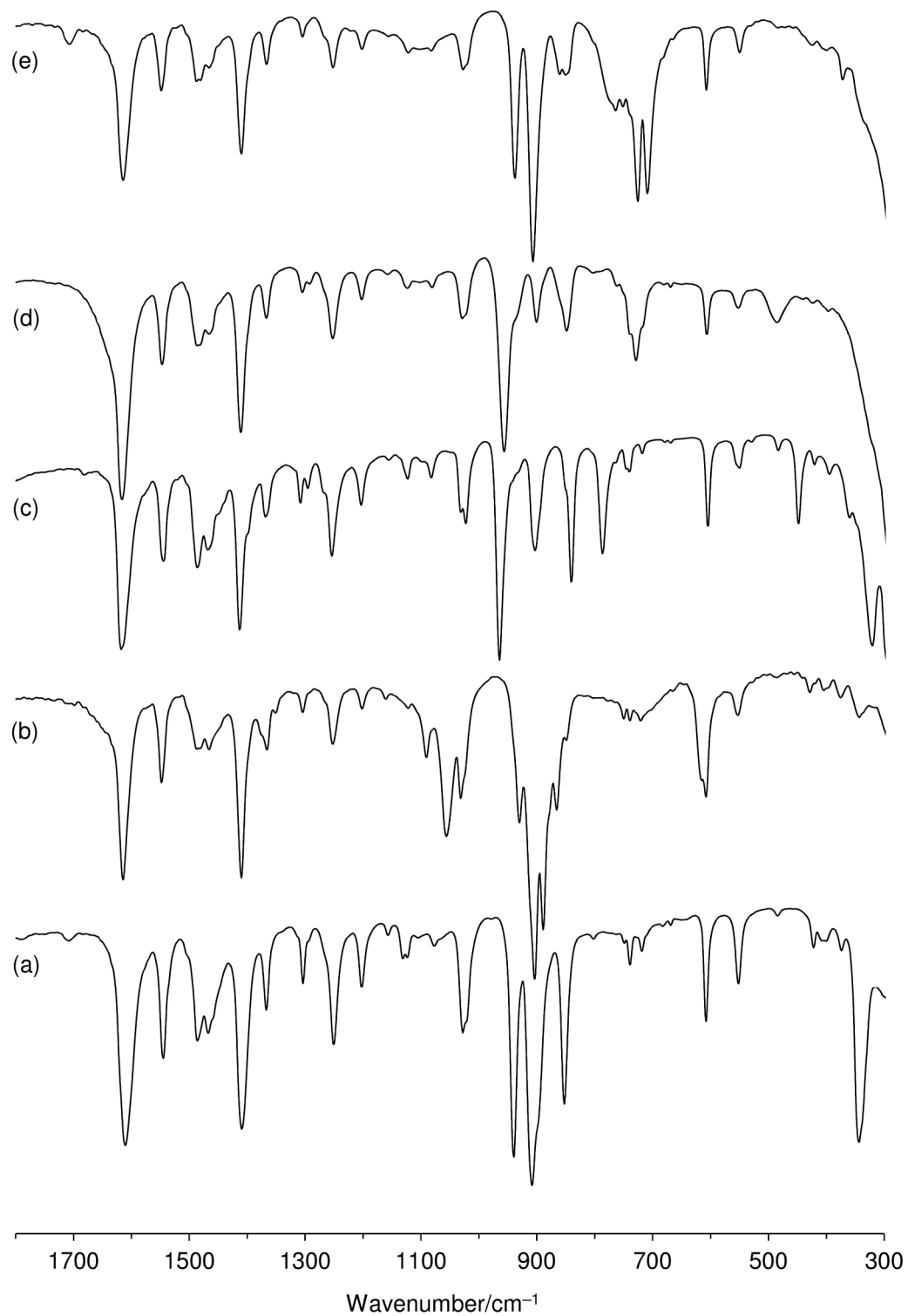


Fig. S2 FT-IR spectra (KBr) in the range 300-1800 cm⁻¹ of complexes (a) **1**, (b) **2**, (c), **3**, (d) **4**, and (e) **5**.

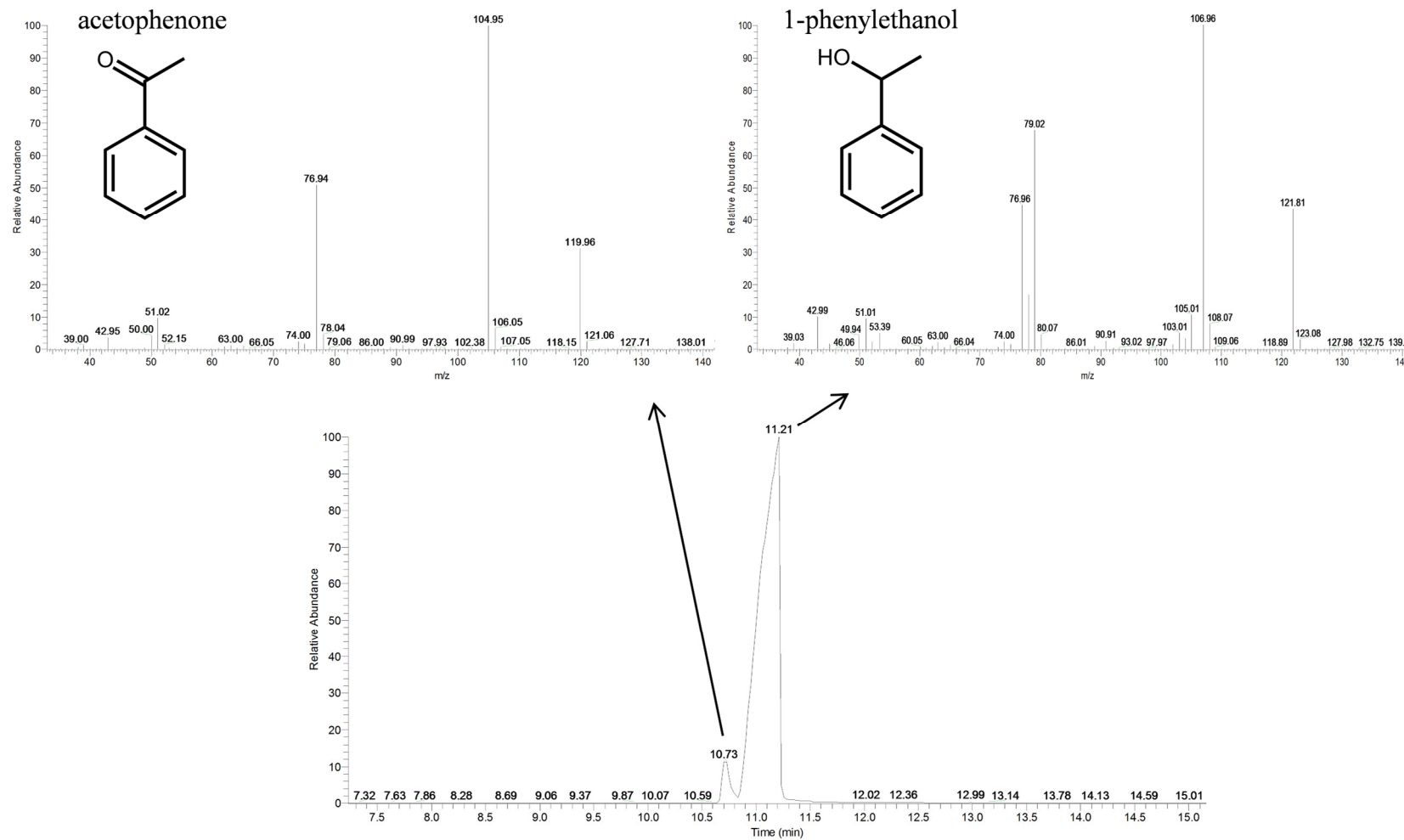


Fig. S3 GC-MS analysis of the solution obtained from the reaction of complex **1** in 1-phenylethanol at 130 °C for 24 h (bottom), and the mass spectra for the chromatographic peaks, which corresponded to acetophenone (top left) and 1-phenylethanol (top right).

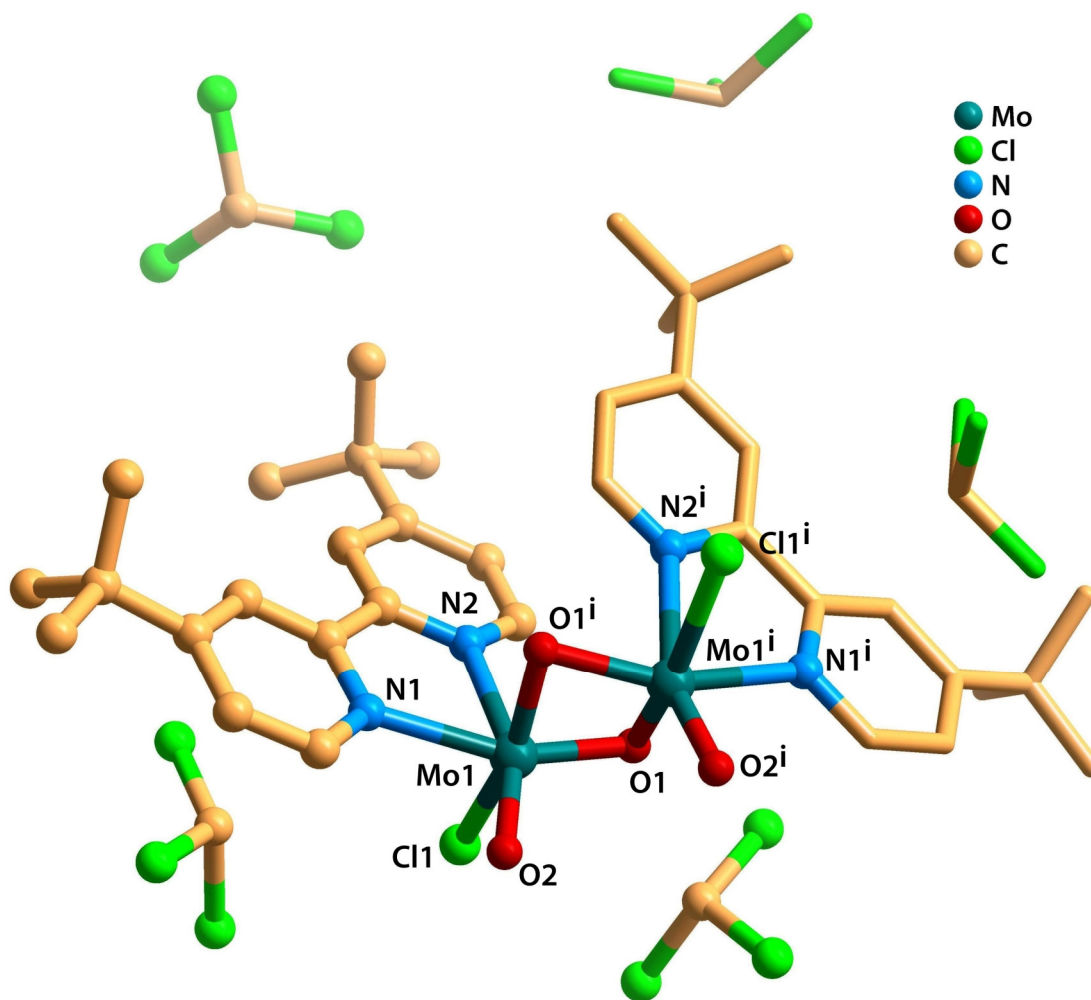


Fig. S4 Crystal structure of the compound $[\text{Mo}_2\text{O}_2(\mu_2\text{-O})_2\text{Cl}_2(\text{di-}t\text{Bu-bipy})_2]\cdot 5\text{CHCl}_3$ (**4**·5CHCl₃), showing the labelling scheme for all atoms composing the Mo coordination environments; elements of the asymmetric unit and first coordination spheres are represented in a ball-and-stick model, and all H-atoms have been omitted for clarity. Detailed information about the bond lengths and angles of the Mo coordination centres is summarised in Table S4.

Description of crystal packing

The crystal packing of the mononuclear complex $[\text{MoO}_2\text{Cl}(\text{OEt})(\text{di-}t\text{Bu-bipy})]$ (**2**) is generally mediated by an extensive network of C–H \cdots O and C–H \cdots Cl weak hydrogen bonds (light blue dashed lines in Figs. S5 and S6; geometric details about hydrogen bonds are summarised in Table S5). These intermolecular interactions lead to the formation of two-dimensional (2D) supramolecular networks (infinite layers) extended in the [1 0 0] direction of the unit cell (Fig. S5a), which close pack along the *a*-axis of the unit cell (Fig. S5b). The cooperative effect of the extensive hydrogen bonding network, as well as the absence of solvent molecules of crystallization, originate an overall solid-state structure that is considerably compact, with no voids or channels.

The solvent molecules of crystallisation reveal a decisive role in the extended crystal packing of the dinuclear complex **4** in both of the structures **4**·2EtOH and **4**·5CHCl₃. In **4**·2EtOH, the solvent molecules interact directly with adjacent complexes by long O–H \cdots Cl hydrogen bonds involving the OH groups of the EtOH molecules and the chlorido ligands of the complex (O5–H5 \cdots Cl2 and O6–H6 \cdots Cl1; see Table S6 for geometric details about the hydrogen bonds). Furthermore, an extensive network of weak C–H \cdots O and C–H \cdots Cl hydrogen bonds between adjacent complexes originates a three-dimensional (3D) supramolecular structure with cavities occupied by the EtOH molecules (Fig. S7).

The recrystallisation of the dinuclear complex **4** from a solution in CHCl₃ rather than EtOH led to a crystal structure with the cubic space group *Fd*-3c and an enormous unit cell [axis of 58.3972(4) Å and volume total of 199148(4) Å³], and a totally distinct extended crystal packing. In compound **4**·5CHCl₃ the neighbouring complex moieties close pack and interact by a large network of weak C–H \cdots O and C–H \cdots Cl hydrogen bonds, originating a 3D hydrogen-bonded framework with high porosity (Fig. S8; hydrogen bonds are not shown; details about the geometry of these interactions are given in Table S7). The large pores and cavities are filled with the CHCl₃ molecules of crystallisation, since the solvent accessible surface was estimated to be ca. 17% of the unit cell (ca. 33630 Å³ per cell; Fig. S9).

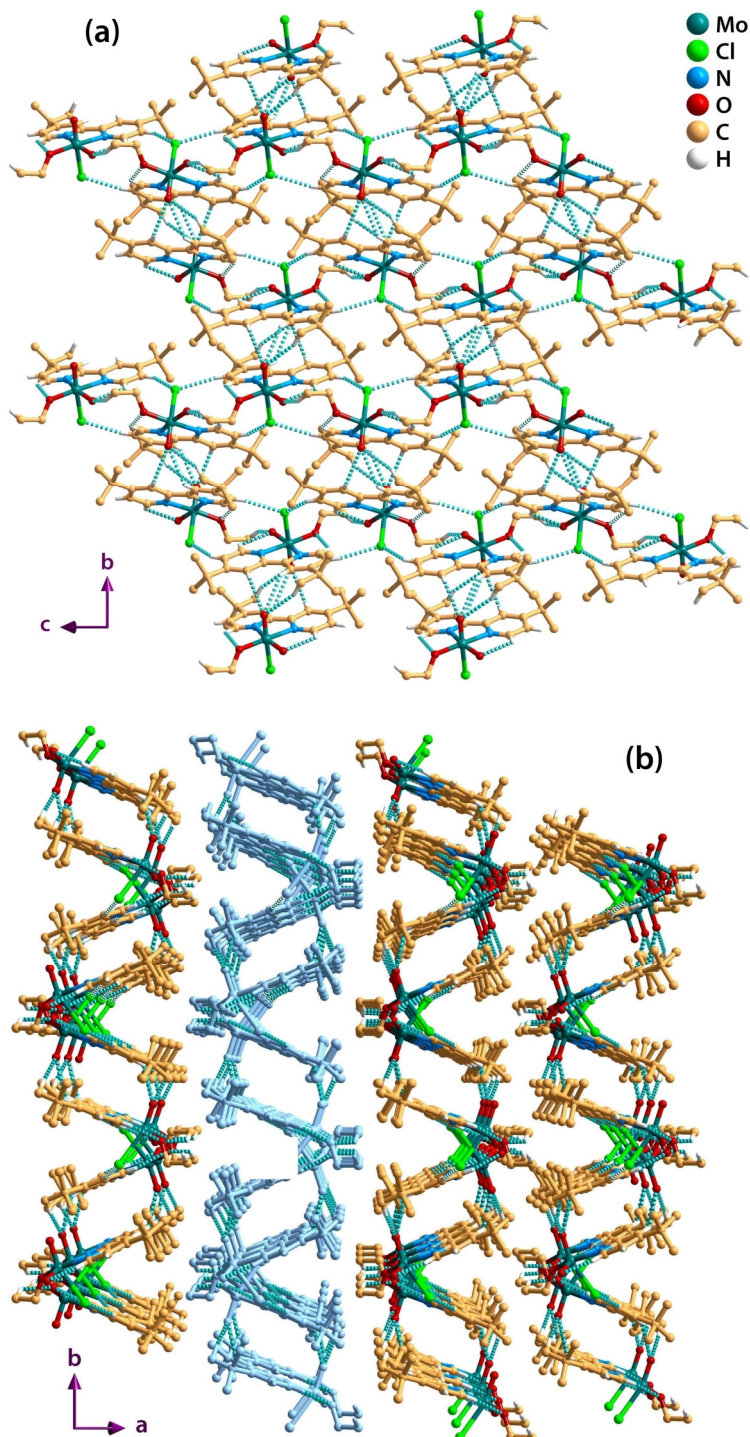


Fig. S5 (a) C–H···O and C–H···Cl interactions between adjacent mononuclear complexes $[\text{MoO}_2\text{Cl}(\text{OEt})(\text{di-}t\text{Bu-bipy})]$ (**2**), originating a 2D hydrogen-bonded network (layers) extended in the *bc* plane of the unit cell. (b) Overall crystalline arrangement viewed in the $[0\ 0\ 1]$ direction of the unit cell, showing the packing of individual supramolecular layers along the *a*-axis of the unit cell (one layer is highlighted in blue). H-atoms have been omitted for clarity, except for those involved in the weak hydrogen bonds (represented as light blue dashed lines); geometric details of these interactions are listed in Table S5.

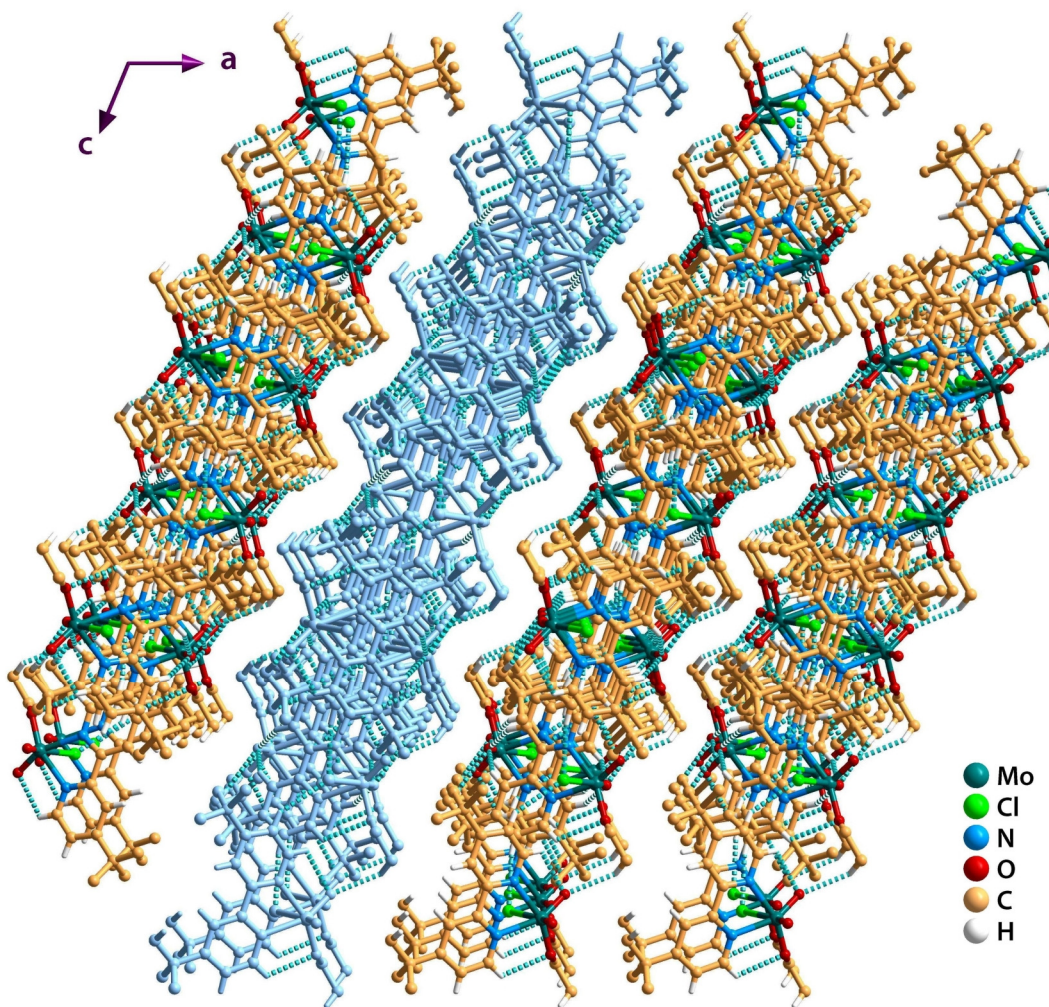


Fig. S6 Crystal packing of the mononuclear complexes $[\text{MoO}_2\text{Cl}(\text{OEt})(\text{di-}t\text{Bu-bipy})]$ (**2**) viewed in the $[0\ 1\ 0]$ direction of the unit cell; weak $\text{C}-\text{H}\cdots\text{O}$ and $\text{C}-\text{H}\cdots\text{Cl}$ hydrogen bonds are represented as dashed blue lines and an individual supramolecular layer is drawn in blue. For clarity, only the H-atoms involved in the hydrogen bonding network are shown.

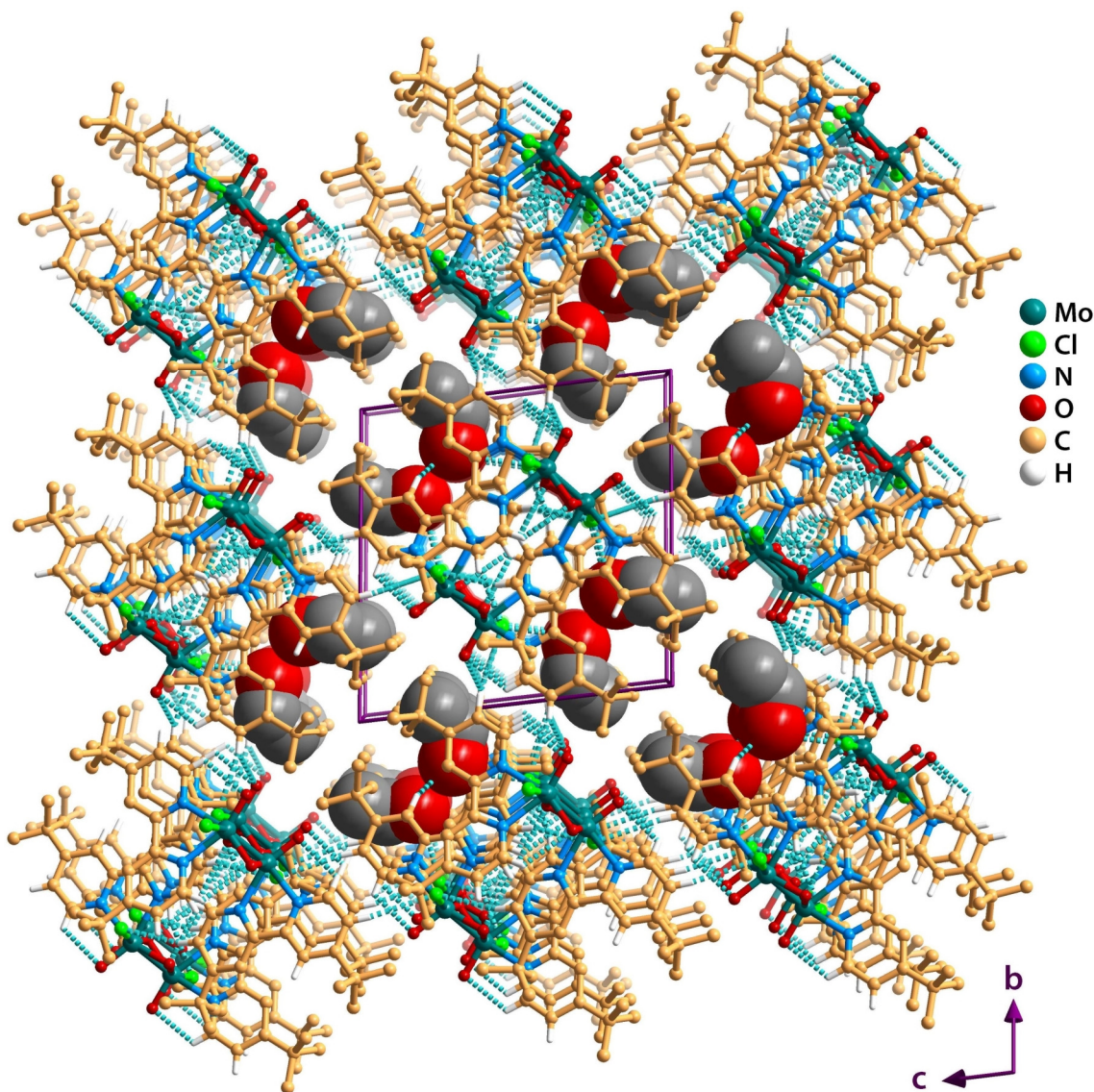


Fig. S7 Crystal packing of $[\text{Mo}_2\text{O}_2(\mu_2-\text{O})_2\text{Cl}_2(\text{di-}t\text{Bu-bipy})_2]\cdot 2\text{EtOH}$ (**4**·2EtOH) viewed in perspective along the $[1\ 0\ 0]$ direction of the unit cell, revealing a 3D hydrogen-bonded framework. Complexes are represented in ball-and-stick mode and the EtOH molecules are displayed in space-filling models, while the hydrogen bonds are drawn as dashed blue lines. For clarity, only the H-atoms involved in these intermolecular interactions are shown. Information about the hydrogen bonds is presented in Table S6.

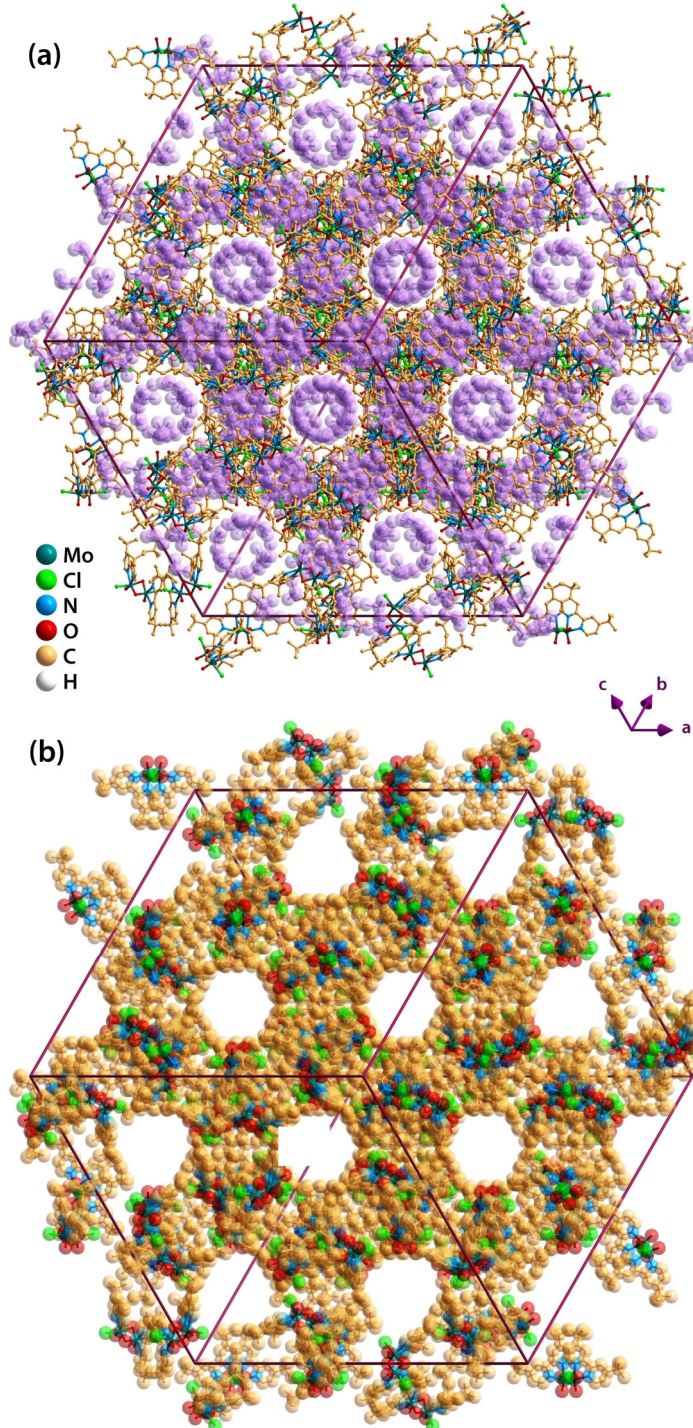


Fig. S8 Extended crystal packing features of $[\text{Mo}_2\text{O}_2(\mu_2\text{-O})_2\text{Cl}_2(\text{di-}t\text{Bu-bipy})_2]\cdot 5\text{CHCl}_3$ (**4**·5CHCl₃): (a) with the pores and cavities filled with the solvent molecules of crystallisation (CHCl₃ drawn in lavender colour and space-filling mode with van der Waals radius of 1 Å); (b) without CHCl₃ molecules, and the atoms of the complexes represented in space-filling mode with van der Waals radius of 1 Å. H-atoms have been omitted for clarity.

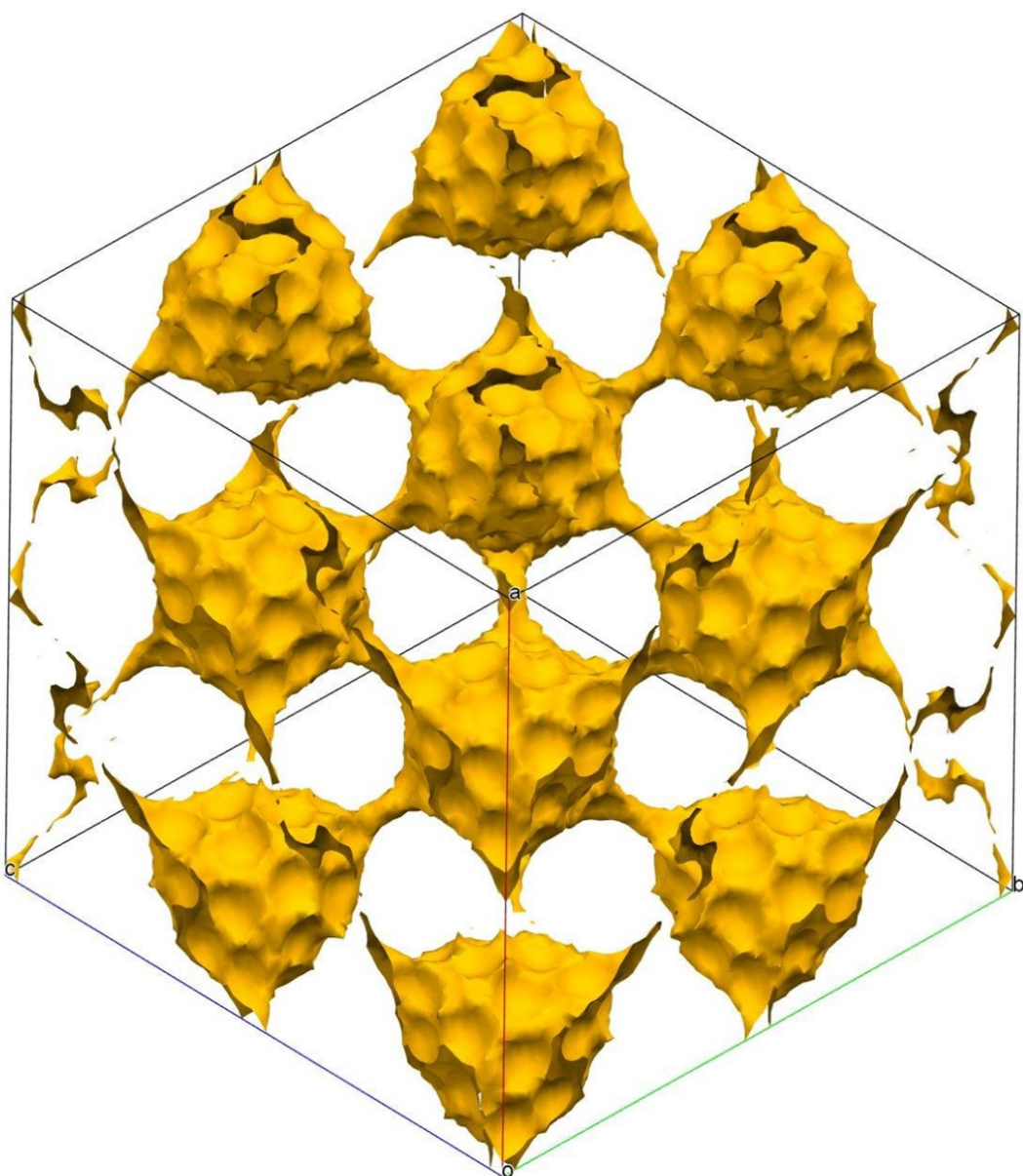


Fig. S9 Representation of the solvent accessible surface in the crystal structure of the compound $[\text{Mo}_2\text{O}_2(\mu_2\text{-O})_2\text{Cl}_2(\text{di-}t\text{Bu-bipy})_2]\cdot 5\text{CHCl}_3$ (**4** \cdot 5CHCl₃), evaluated with the program Mercury.

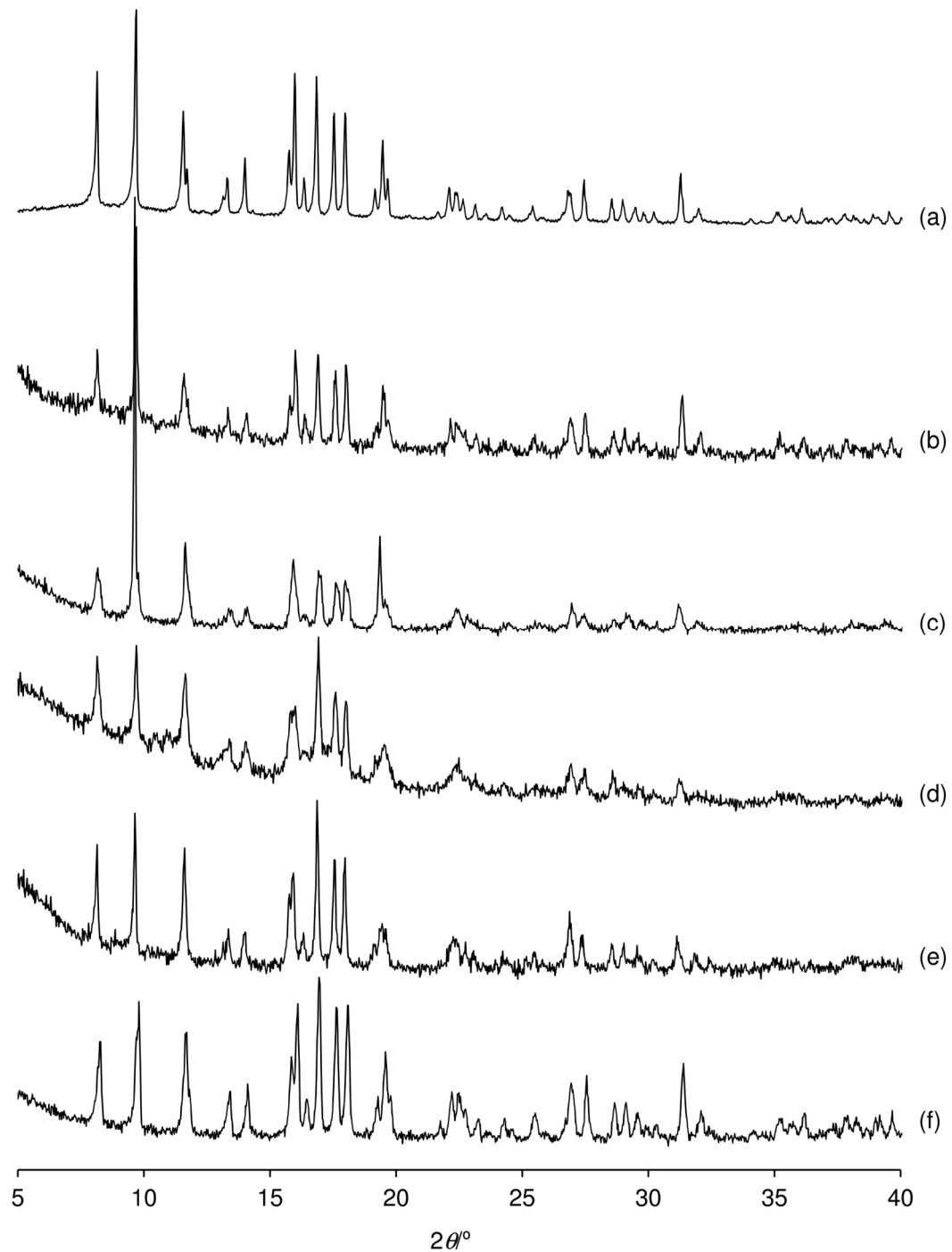


Fig. S10 Powder XRD patterns of (a) complex **1**, (b) **1**/BzA-liq, (c) **1**/BzA-sol, (d) **1**/CT-sol, (e) **1**/PhEtOH-liq, and (f) **1**/PhEtOH-sol.

Table S1 Crystal and structure refinement data for $[\text{MoO}_2\text{Cl}(\text{OEt})(\text{di-}t\text{Bu-bipy})]$ (**2**), $[\text{Mo}_2\text{O}_2(\mu_2\text{-O})_2\text{Cl}_2(\text{di-}t\text{Bu-bipy})_2] \cdot 2\text{EtOH}$ (**4·2EtOH**) and $[\text{Mo}_2\text{O}_2(\mu_2\text{-O})_2\text{Cl}_2(\text{di-}t\text{Bu-bipy})_2] \cdot 5\text{CHCl}_3$ (**4·5CHCl₃**)

	2	4·2EtOH	4·5CHCl₃
Chemical formula	$\text{C}_{20}\text{H}_{29}\text{ClMoN}_2\text{O}_3$	$\text{C}_{40}\text{H}_{60}\text{Cl}_2\text{Mo}_2\text{N}_4\text{O}_6$	$\text{C}_{41}\text{H}_{53}\text{Cl}_7\text{Mo}_2\text{N}_4\text{O}_4$
M_r	476.84	955.70	1460.40
Crystal description	Yellow blocks	Orange blocks	Orange prism
Crystal size/mm	$0.08 \times 0.06 \times 0.03$	$0.09 \times 0.05 \times 0.02$	$0.19 \times 0.18 \times 0.11$
Crystal system, space group	Monoclinic, $P2_1/c$	Triclinic, P-1	Cubic, $Fd-3c$
$a/\text{\AA}$	10.9605(7)	12.2348(8)	58.3972(4)
$b/\text{\AA}$	15.9334(10)	14.0396(9) \AA	58.3972(4)
$c/\text{\AA}$	13.4384(8)	14.2351(10)	58.3972(4)
$\alpha/^\circ$	90	92.035(3)	90
$\beta/^\circ$	112.447(2)	107.553(3)	90
$\gamma/^\circ$	90	104.751(3)	90
Volume/ \AA^3	2169.0(2)	2237.7(3)	199148(4)
Z	4	2	96
$\rho_{\text{calculated}}/\text{g cm}^{-3}$	1.460	1.418	1.169
$F(000)$	984	988	70272
μ/mm^{-1}	0.746	0.726	0.879
θ range/ $^\circ$	3.933 to 25.024	3.863 to 25.027	3.742 – 25.025
Index ranges	$-11 \leq h \leq 13$ $-18 \leq k \leq 15$ $-15 \leq l \leq 15$	$-13 \leq h \leq 14$ $-15 \leq k \leq 16$ $-16 \leq l \leq 16$	$-67 \leq h \leq 69$ $-69 \leq k \leq 61$ $-69 \leq l \leq 69$
Reflections collected	13846	22401	302253
Independent reflections	3796 ($R_{\text{int}} = 0.0409$)	7815 ($R_{\text{int}} = 0.0499$)	7298 ($R_{\text{int}} = 0.1231$)
Final R indices [$I > 2\sigma(I)$]	$R_1 = 0.0464$ $wR_2 = 0.1008$	$R_1 = 0.0447$ $wR_2 = 0.0956$	$R_1 = 0.0545$ $wR_2 = 0.1472$
Final R indices (all data)	$R_1 = 0.0718$ $wR_2 = 0.1116$	$R_1 = 0.0722$ $wR_2 = 0.1070$	$R_1 = 0.0843$ $wR_2 = 0.1751$
$\Delta\rho_{\text{max}}$ and $\Delta\rho_{\text{min}}/\text{e\AA}^{-3}$	1.286 and -0.664	1.105 and -0.493	1.330 and -0.56

Table S2 Selected bond lengths (in Å) and angles (in degrees) for the Mo coordination centre observed in complex **2**, [MoO₂Cl(OEt)(di-*t*Bu-bipy)].

Mo1–O2	1.633(3)	O1–Mo1–O2	104.9(2)
Mo1–O1	1.699(5)	O1–Mo1–O3	106.8(2)
Mo1–O3	1.882(3)	O1–Mo1–N1	88.77(19)
Mo1–N1	2.253(4)	O1–Mo1–N2	154.9(2)
Mo1–N2	2.316(3)	O1–Mo1–Cl1	89.46(18)
Mo1–Cl1	2.5734(12)	O2–Mo1–O3	100.49(15)
		O2–Mo1–N1	89.73(13)
		O2–Mo1–N2	88.34(13)
		O2–Mo1–Cl1	161.06(9)
		O3–Mo1–N1	158.18(13)
		O3–Mo1–N2	91.12(12)
		O3–Mo1–Cl1	86.69(11)
		N1–Mo1–N2	69.79(11)
		N1–Mo1–Cl1	78.11(10)
		N2–Mo1–Cl1	73.91(9)

Table S3 Selected bond lengths (in Å) and angles (in degrees) for the Mo coordination centres in compound **4**·2EtOH, $[\text{Mo}_2\text{O}_2(\mu_2\text{-O})_2\text{Cl}_2(\text{di-}t\text{Bu-bipy})_2]\cdot 2\text{EtOH}$.

Mo1–O1	1.687(3)	Mo2–O4	1.687(3)
Mo1–O3	1.913(3)	Mo2–O2	1.917(3)
Mo1–O2	1.947(3)	Mo2–O3	1.945(3)
Mo1–N1	2.235(3)	Mo2–N4	2.229(3)
Mo1–N2	2.319(3)	Mo2–N3	2.303(3)
Mo1–Cl1	2.4889(12)	Mo2–Cl2	2.4906(12)
O1–Mo 1–O2	106.60(13)	O2–Mo2–O3	91.70(11)
O1–Mo1–O3	112.05(12)	O2–Mo2–O4	112.04(13)
O1–Mo1–N1	89.13(13)	O2–Mo2–N3	88.02(11)
O1–Mo1–N2	156.45(13)	O2–Mo2–N4	157.85(12)
O1–Mo1–Cl1	91.55(10)	O2–Mo2–Cl2	89.03(9)
O2–Mo1–O3	91.74(12)	O3–Mo2–O4	106.52(13)
O2–Mo1–N1	83.63(12)	O3–Mo2–N3	83.27(12)
O2–Mo1–N2	83.59(12)	O3–Mo2–N4	84.17(12)
O2–Mo1–Cl1	159.94(8)	O3–Mo2–Cl2	160.30(9)
O3–Mo1–N1	158.73(12)	O4–Mo2–N3	156.90(13)
O3–Mo1–N2	88.27(12)	O4–Mo2–N4	89.95(13)
O3–Mo1–Cl1	89.17(9)	O4–Mo2–Cl2	91.39(10)
N1–Mo1–N2	70.61(12)	N3–Mo2–N4	69.91(12)
N1–Mo1–Cl1	88.29(9)	N3–Mo2–Cl2	77.07(9)
N2–Mo1–Cl1	76.41(9)	N4–Mo2–Cl2	87.76(9)

Table S4 Selected bond lengths (in Å) and angles (in degrees) for the Mo coordination centre in compound **4**·5CHCl₃, [Mo₂O₂(μ₂-O)₂Cl₂(di-*t*Bu-bipy)₂]·5CHCl₃.^a

Mo1–O2	1.686(3)	O1–Mo1–O2	113.25(15)
Mo1–O1	1.926(3)	O1–Mo1–O1 ⁱ	92.29(13)
Mo1–O1 ⁱ	1.948(3)	O1–Mo1–N1	154.95(14)
Mo1–N1	2.211(4)	O1–Mo1–N2	84.84(13)
Mo1–N2	2.317(7)	O1–Mo1–Cl1	87.54(10)
Mo1–Cl1	2.4761(13)	O2–Mo1–O1 ⁱ	105.73(15)
		O2–Mo1–N1	91.78(16)
		O2–Mo1–N2	157.93(15)
		O2–Mo1–Cl1	91.83(12)
		O1 ⁱ –Mo1–N1	81.36(14)
		O1 ⁱ –Mo1–N2	85.13(13)
		O1 ⁱ –Mo1–Cl1	160.87(10)
		N1–Mo1–N2	70.55(14)
		N1–Mo1–Cl1	90.75(11)
		N2–Mo1–Cl1	75.80(10)

^aSymmetry transformation used to generate equivalent atoms:

(i) $x+1/4, -y+2, z-1/4$

Table S5 Hydrogen bonding geometry (distances in Å and angles in degrees) for complex **2**, [MoO₂Cl(OEt)(di-*t*Bu-bipy)].^a

C–H…A	<i>d</i> (H…A)	<i>d</i> (C…A)	∠(CHA)
C2–H2…O3	2.65	3.173(5)	116.6
C3–H3…Cl1 ⁱ	2.76	3.665(4)	165.1
C5–H5…O2 ⁱⁱ	2.76	3.429(5)	129.2
C8–H8…O1	2.50	2.992(7)	113.5
C9–H9…Cl1 ⁱⁱⁱ	2.82	3.617(4)	144.9
C15–H15…O2 ⁱⁱ	2.72	3.473(6)	138.6
C17–H17b…O2 ⁱⁱ	2.82	3.726(4)	157.8
C22–H22B…O1 ⁱ	2.57	3.344(7)	138.1

^aSymmetry transformation used to generate equivalent atoms:

(i) $x, -y+1/2, z-1/2$; (ii) $-x+1, -y, -z+1$; (iii) $x, -y+1/2, z+1/2$.

Table S6 Hydrogen bonding geometry (distances in Å and angles in degrees) for compound **4**·2EtOH, [Mo₂O₂(μ₂-O)₂Cl₂(di-*t*Bu-bipy)₂]·2EtOH.^a

D–H···A	d (H···A)	d (D···A)	∠(DHA)
O5–H5···Cl2	2.47(3)	3.356(4)	157(5)
O6–H6···Cl1	2.434(18)	3.365(4)	167(6)
C1–H1···O1	2.46	2.968(5)	113.1
C2–H2···Cl1 ⁱ	2.97	3.900(5)	167.6
C4–H4···O5 ⁱⁱ	2.52	3.376(6)	150.8
C13–H13···Cl1 ⁱⁱⁱ	2.90	3.828(5)	164.7
C14–H14···O3	2.62	3.144(5)	115.4
C19–H19···O2	2.56	3.098(5)	115.8
C20–H20···Cl2 ⁱⁱ	2.85	3.776(4)	164.1
C31–H31···Cl2 ^{iv}	2.87	3.785(4)	161.9
C32–H32···O4	2.45	2.964(5)	113.9

^a Symmetry transformation used to generate equivalent atoms:

- (i) $-x+1, -y+1, -z$; (ii) $-x+2, -y+1, -z+1$; (iii) $-x+1, -y+1, -z+1$;
- (iv) $-x+2, -y+2, -z+1$

Table S7 Hydrogen bonding geometry (distances in Å and angles in degrees) for compound **4**·5CHCl₃, [Mo₂O₂(μ₂-O)₂Cl₂(di-*t*Bu-bipy)₂]·5CHCl₃.^a

C–H···A	d (H···A)	d (C···A)	∠(CHA)
C1–H1···O2	2.50	3.007(6)	113.6
C1–H1···Cl4 ⁱⁱ	2.91	3.789(6)	155.1
C4–H4···Cl1 ⁱⁱⁱ	2.79	3.741(5)	179.4
C11–H11···Cl1 ⁱⁱⁱ	2.71	3.627(5)	161.5
C14–H14···O1	2.46	3.007(6)	116.2
C19–H19···O2 ⁱⁱⁱ	2.29	3.195(8)	150.6
C20–H20···Cl1	2.86	3.691(7)	140.5
C20–H20···O1	2.23	3.117(6)	146.5
C21–H21···Cl1 ⁱⁱⁱ	2.67	3.572(11)	150.4

^a Symmetry transformation used to generate equivalent atoms:

- (ii) $x+3/4, y-3/4, -z+1/2$; (iii) $-x+1/2, y-3/4, z+3/4$.